SPANDIDOS PUBLICATIONS EXPERIMENTAL AND THERAPEUTIC MEDICINE 14: 4755-4760, 2017

In vivo and *in vitro* studies on the roles of p38 mitogen-activated protein kinase and NADPH-cytochrome P450 reductase in Alzheimer's disease

YUNYI YAO[1,2], JIN-ZHONG HUANG[3], LIANG CHEN[4], YINGQI CHEN[5] and XIANHONG LI[3]

[1]Department of Biochemistry, Xuzhou Medical University, Xuzhou, Jiangsu 221004; [2]Department of Medical Technology, Suzhou Vocational Health College, Suzhou, Jiangsu 215009; [3]Department of Neurology, The Third Affiliated Hospital of Soochow University, Changzhou, Jiangsu 213000; [4]Department of Pediatrics, Changhai Hospital, The Second Military Medical University, Shanghai 200433; [5]Department of Neurology, Suzhou Hospital of Traditional Chinese Medicine, Suzhou, Jiangsu 215009, P.R. China

Received October 17, 2016; Accepted June 29, 2017

DOI: 10.3892/etm.2017.5182

Abstract. Alzheimer's disease (AD) is a chronic neurodegenerative disease with an increasing morbidity rate. As one of the most important signaling pathways that responds to inflammation and degeneration, the p38 mitogen-activated protein kinase (MAPK) signaling pathway is active in the cortexes of AD mice. At the cellular level the same effect can be observed with p38 MAPK when induced by amyloid β $(Aβ)_{1-42}$, a 42-residue Aβ fragment. Inhibition of p38 MAPK in the present study protected SH-SY5Y cells from the toxicity of $Aβ_{1-42}$, and alleviated the formation of senile plaques and cognitive impairment in AD mice. The expression of cytochrome P450 reductase (CPR) in the brains of mice with AD, in addition to $Aβ_{1-42}$-treated SH-SY5Y cells, also increased. However, the inhibition of CPR did not protect SH-SY5Y cells from the toxicity of $Aβ_{1-42}$. The results of the present study suggest that p38 MAPK is a potential therapeutic target for the treatment of AD. In addition, the main enzyme that metabolizes drugs, CPR, could serve a more complex role in AD.

Introduction

Alzheimer's disease (AD), first described and termed by the German psychiatrist and pathologist Alois Alzheimer in 1906, is a chronic neurodegenerative disease and a form of dementia (1,2). There are ~47 million patients with dementia worldwide with 9.9 million new cases every year, in which 60-80% of dementia cases are AD (2). In AD, the patient's mental and physical condition declines, including problems with language, orientation, memory and motivation, ultimately leading to mortality (2,3). Senile plaques are one of the most important pathological features of AD. AD is highly associated with senile plaques due to the accumulation of amyloid β (Aβ) protein (4). Besides increasing age and certain genetic risks, AD is associated with inflammatory cytokines, vascular diseases and cholesterol levels (5-7). Currently, a number of medications or supplements can efficiently attenuate the progression or decrease the risk of developing AD (8).

p38 mitogen-activated protein kinase (MAPK) is responsive to stress stimuli, including inflammation, cytokines, radiation and shock, and is involved in cell proliferation, differentiation, apoptosis and autophagy. Given that AD is a neurodegenerative disease associated with inflammation and cytokines (5,9), investigating the role of p38 MAPK will aid in the understanding of the underlying mechanisms of AD. Cytochromes P450 (CYPs; max absorption, 450 nm) is a superfamily of the terminal oxidase enzymes that are present in electron transfer chains, in which electrons are transferred from NADPH to CYPs via cytochrome P450 reductase (CPR). CYPs are involved in the majority of chemical metabolism (deactivation or activation) that occurs in the body. Certain chemicals can change the biosynthesis or activity of CYPs, which then affects the metabolism and clearance of other compounds (10,11). Although certain CYPs have been reported to be abnormally expressed in AD (12-14), reports on CPR are limited.

In the present study, *in vivo* and *in vitro* studies were performed to investigate the role of p38 MAPK and CPR in AD. The results of the present study may aid in the understanding of the mechanisms of and potential treatments for AD.

Materials and methods

Control mice and mouse models of AD. APPswe/PSEN1dE9 (AD) male mice (weighing 24±3 g at 9 months old), originally

Correspondence to: Dr Yunyi Yao, Department of Biochemistry, Xuzhou Medical University, 209 Tongshan Road, Xuzhou, Jiangsu 221004, P.R. China
E-mail: yaoyunyiyyy@126.com

Key words: Alzheimer's disease, amyloid $β_{1-42}$, p38 mitogen-activated protein kinase, apoptosis, NADPH-cytochrome P450 reductase

generated in Jackson Laboratory (Bar Harbor, ME USA), were purchased from the Model Animal Research Center of Nanjing University (Nanjing, China); age- and sex-matched wild-type (WT) C57BL/6J male mice (weighing 22±2 g) were also were purchased from Model Animal Research Center of Nanjing University and used as negative controls. A total of 36 mice, 21 AD mice and 15 WT mice were used. Among which, 9 AD and 3 WT mice were treated with SB203580 (named as AD + SB and WT + SB separately). The mice were raised in an environment with a temperature of 24±2˚C, humidity of 55±15%, and access to a 12-h light/dark cycle. Mice were given *ad libitum* access to food and water. Experiments and surgeries on the mice were performed according to the Institutional Animal Care and Use Committee (IACUC) guidelines. The animal experiments were approved by and performed in the Animal Research Center of Suzhou Vocational Health College (Suzhou, China).

Senile plaque staining and determination of contextual memory. A total of 12 mice were selected in the senile plaque study. A total of 3 WT mice and 3 AD mice were treated with SB203580 (10 mg/kg; intraperitoneal injection; Sigma-Aldrich; Merck KGaA; Darmstadt, Germany) every 3 days for 30 days starting at the 9-month time point, experiments were then performed at the 10-month time point. There was a total of four groups of 10-month-old mice, as follows: WT, AD, WT + SB and AD + SB (3 mice in each group). Brain damage in the AD mice was tested using Thioflavin S (Sigma-Aldrich; Merck KGaA) staining. Mice were euthanized by exposing them to CO_2 following the IACUC guidelines, the brains were then dissected and embedded in optimum cutting temperature compound, and frozen on dry ice. The coronal sections of the mouse brains were cut into 10-μm-thick sections, placed onto slides, and then fixed in 4% paraformaldehyde (PFA) at room temperature for 20 min. The slides were placed in 1% Thioflavin S solution at room temperature for 20 min and then differentiated twice in 70% fresh alcohol for 7 min. Images were captured using a confocal microscope (magnification, x100) and analyzed by calculating the relative area of staining using ImageJ software (National Institutes of Health, Bethesda, MD, USA).

The contextual memory of the mice was examined using a fear-conditioning assay modified from a previous study (15). A total of 6 WT mice, 6 AD mice and 6 AD + SB mice were used for the contextual memory study. Freezing tests were performed in four chambers (17.8x19.1x38.1 cm). The session began with the house light on. Firstly, mice were exposed to 5 conditioned stimuli (30 sec, 85 dB, white noise), followed by a 30-sec trace period and treatment with the unconditioned stimulus (2 sec, 0.285-mA foot-shock) paired with a 5-sec tone in the chambers on the first day. On the second day, mice were placed in the chambers to test for freezing for a total of 5 min. Freezing time in the absence of foot-shock and tone in the first 2.5 min and with the tone in the later 2.5 min were recorded. Relative memory deficit was calculated as the percentage of freezing condition (absence of all non-respiratory movements) as follows: Freezing time/Total test time x100%.

Detection of p-p38 MAPK and CPR in mouse cortexes by western blot analysis. phospho (p)-p38 MAPK and CPR were detected in the cortexes of the brains of 3 WT mice and 3 AD mice. Microsomes were obtained and isolated from the cortexes; these subcellular fractions were used to detect the expression of CPR. The cortex was homogenized on ice in 10 mM PBS (pH, 7.7) containing 250 mM sucrose, 1 mM EDTA and 0.5 mM phenylmethylsulfonyl fluoride for 15 sec, then centrifuged for 20 min at 10,000 x g at 4˚C. The supernatant was collected and centrifuged for 1 h at 40,000 x g at 4˚C, then the supernatant was decanted. The pellet was resuspended in 0.1 M PBS containing 1 mM EDTA, 1 mM dithiothreitol, 30% glycerol and protease inhibitors (pH, 7.25). Protein was also extracted from the mouse cortexes and homogenized in protein extraction buffer containing 0.5 mM phenylmethylsulfonyl fluoride, 80 μg/ml DL-dithiothreitol. Protein was boiled for 5 min, cooled on ice for 1 min and then centrifuged for 1 min at 10,000 x g at 4˚C. Both microsome and protein were quantified using BCA Protein Assay (Thermo Scientific, Rockford, IL, USA). A total of 10 μg microsome or 25 μg protein were injected into each lane then separated via SDS-PAGE on a 12.5% gel and transferred onto a polyvinylidene difluoride membrane. The membranes were blocked in 5% fat-free milk for 1 h at room temperature, then incubated overnight at 4˚C with a primary rabbit polyclonal IgG antibodies directed against p-p38 MAPK (Thr180/Tyr182; cat no: 9211; 1:1,000; Cell Signaling Technology, Inc., Danvers, MA, USA) or CPR (cat. no. ab13513; 1:1,000; Abcam, Cambridge, UK). Subsequently, secondary anti-rabbit goat IgG antibodies (cat. no. A16110; 1:4,000; Thermo Fisher Scientific, Inc., Carlsbad, CA, USA) were applied for 2 h at room temperature. GAPDH (cat. no. G9545; 1:2,000; Sigma-Aldrich, Merck KGaA) was used as internal control for protein detection.

Detection of p-p38 MAPK and CPR in SH-SY5Y cells. The human neuroblastoma cell line, SH-SY5Y, was purchased from the Type Culture Collection of the Chinese Academy of Sciences (Shanghai, China). The cells were cultured in a 1:1 mixture of DMEM and Ham's Nutrient Mixture F12 medium (both HyClone™; GE Healthcare, Logan, UT, USA) supplemented with 10% fetal bovine serum (Shanghai ExCell Biology, Inc., Shanghai, China), 100 U/ml penicillin and 0.1 mg/ml streptomycin (HyClone; GE Healthcare). The sequence of the $A\beta_{1-42}$ peptide (molecular weight, 4514.08 kDa; Sangon Biotech Co., Ltd., Shanghai, China) was DAEFRHDSGYEVHHQKL VFFAEDVGSNKGAIIGLMVGGVVIA. $A\beta_{1-42}$ was dissolved in dimethyl sulfoxide, giving a concentration of 1 mM; 100 μl of this solution and 900 μl PBS was then mixed to generate a 100 μM $A\beta_{1-42}$ solution. The product was incubated at 37˚C for 7 days prior to usage. SH-SY5Y cells were treated with 10 μM $A\beta_{1-42}$ for 48 h prior to the detection of p-p38 MAPK in the cell lysate (previously subjected ice-cold cell lysis buffer before the pellet was resuspended, incubated on ice for 10 min, centrifuged at 20,817 x g for 15 min at 4˚C and the supernatant was collected) and CPR in microsomes by western blotting as described above.

Cell viability and apoptosis assays. MTT assays were performed to detect the viability of SH-SY5Y cells, which were seeded at a density of 3,000 cells/well in 96-well plates and cultured with 10 μM $A\beta_{1-42}$ for 72 h. The expression of

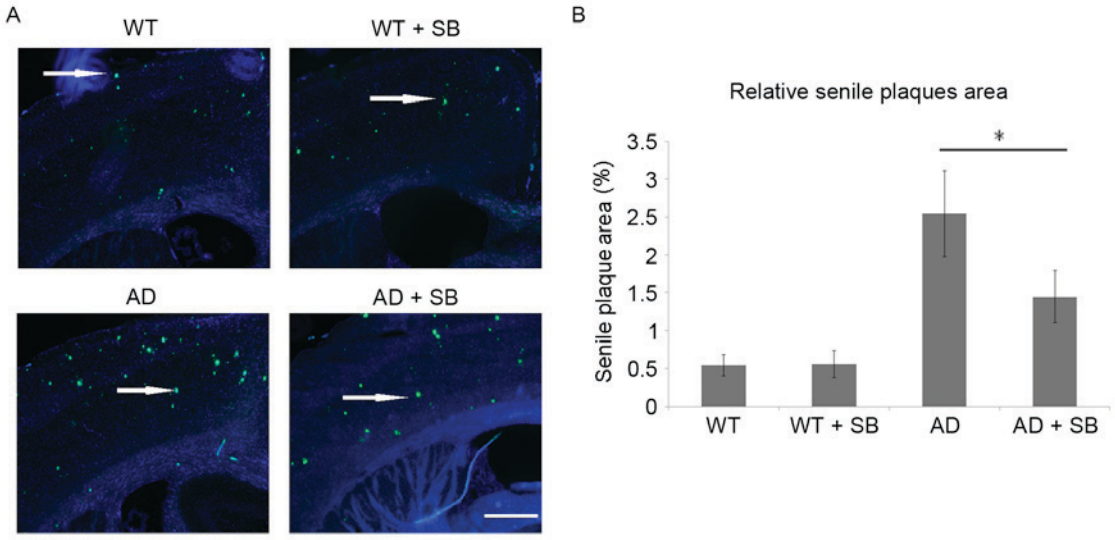

Figure 1. Inhibition of p38 mitogen-activated protein kinase decreases senile plaques in mice with AD. (A) Senile plaque formation (green dots indicated by white arrows) in the cortex of the brains of mice in the four groups. Scale bar, 100 μm; magnification, x100. (B) Relative area of senile plaques in the total section area. *P<0.05. WT, wild-type; SB, SB203580; AD, Alzheimer's disease.

p38 MAPK and CPR was inhibited using the following inhibitors: 3 μM SB203580 (SB) (Sigma-Aldrich; Merck KGaA) and 80 μM tannic acid (TA) (Sigma-Aldrich; Merck KGaA), respectively. For the proliferation assay, 20 μl of 5 mg/ml MTT (Beyotime Institute of Biotechnology, Haimen, China) was added to each well and the plates were incubated at 37˚C for 4 h. The medium was decanted and the cells were incubated with 150 μl formazan solution at 37˚C for 15 min. The absorbance of the wells at 590 nm in four groups (WT, 10 μM $A\beta_{1-42}$, 10 μM $A\beta_{1-42}$ + SB203580 and 10 μM $A\beta_{1-42}$ + TA) was then measured. Cell viability in WT group was set as 100%, data in other groups were calculated by comparison.

Staining with 4',6-diamidino-2-phenylindole (DAPI; Beyotime Institute of Biotechnology) was performed to detect apoptotic cells. Subsequent to fixing with 4% PFA for 20 min and 1X PBS/0.5% Triton X-100 for 10 min on ice, the cells were stained with DAPI solution at room temperature for 15 min. Images were captured using a fluorescence microscope (Eclipse Ti-S; Nikon Corporation, Tokyo, Japan) at a magnification of x200. Caspase-3 activity was detected using Caspase 3 Activity Assay kit (Beyotime Biotechnology), according to the manufacturer's protocol. A total of 10 μl of 2 mM Ac-DEVD-pNA, a caspase-3 substrate that hydrolyzes to pNA, was added to the SH-SY5Y cell culture, which was then incubated for 2 h at 37˚C. The absorbance of pNA at 405 nm was subsequently measured. The activity of caspase-3 was normalized to the total concentration of protein in the lysates and expressed as the relative value. The negative control (NC) group consisted of untreated cells was set as 1.

Statistical analysis. Data are presented as the mean ± standard deviation, and were analyzed using SPSS software (version 16.0; SPSS, Inc., Chicago, IL, USA). Results were evaluated using the Student's t-test for two groups or one-way analysis of variance followed by a post hoc Dunnett's test for multiple groups. P<0.05 was considered to indicate a statistically significant difference.

Results

Inhibition of p38 MAPK decreases the relative senile plaque area in the brains of mice with AD. Senile plaques in mouse cortexes on the hippocampal side were detected using Thioflavin S staining and the relative area of senile plaques in the whole section was evaluated (Fig. 1). A number of senile plaques were detected in the WT and WT + SB groups with no obvious differences. The area of senile plaques increased markedly in the AD group compared with the WT group, indicating senile plaque formation and accumulation. Inhibition of p38 MAPK with SB203580 significantly decreased the area of senile plaques in these AD mice (P<0.05; Fig. 1B).

Expression of p-p38 MAPK and CPR is decreased in AD mice and $A\beta_{1-42}$-treated SH-SY5Y cells. p-p38 MAPK and CPR in mouse brain cortexes and cells were detected by western blot analyses. p-p38 and CPR were notably upregulated in the mice brain cortex in the AD group compared with the WT group (Fig. 2A). p-p38 and CPR were also upregulated in SY-SH5Y cells treated with 10 μM $A\beta_{1-42}$ compared with untreated cells (Fig. 2B). The expression levels of p-p38 and CPR decreased following the treatment with their respective inhibitors (Fig. 2C). These results indicate that CPR and p38 MAPK serve complex roles in AD.

Neuroblastoma cell viability is inhibited by $A\beta_{1-42}$, but this is attenuated by p38 MAPK inhibition. The viability of SH-SY5Y cells was significantly inhibited due to neural toxicity following 10 μM $A\beta_{1-42}$ treatment (P<0.01 vs. the NC group; Fig. 3). Following the inhibition of p38 MAPK with SB203580, the viability of SH-SY5Y cells treated with $A\beta_{1-42}$ significantly increased compared with the 10 μM $A\beta_{1-42}$ alone group (P<0.05; Fig. 3). No significant differences were identified in the $A\beta_{1-42}$ + TA group compared with the $A\beta_{1-42}$ group. Thus, no protection was identified when CPR was inhibited.

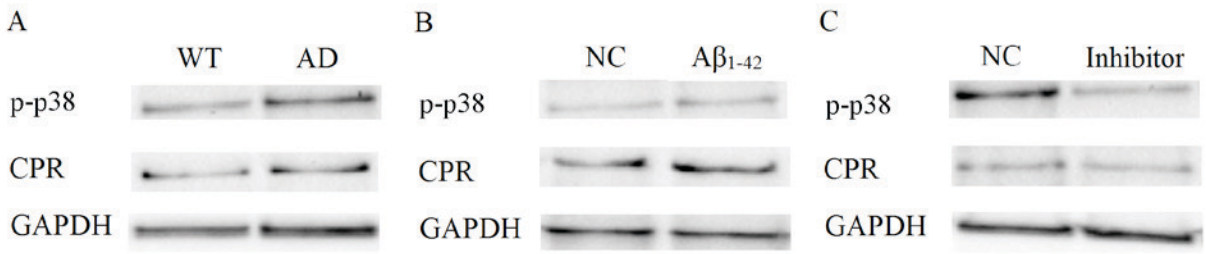

Figure 2. p38 MAPK and CPR are upregulated in AD mice and SH-SY5Y cells treated with $A\beta_{1-42}$. The protein expression of p-p38 MAPK, CPR and GAPDH in (A) WT and AD mice, (B) SH-SY5Y cells in the absence and presence of $A\beta_{1-42}$, and (C) SH-SY5Y cells in the absence and presence of SB203580 or tannic acid. WT, wild-type; AD, Alzheimer's disease; NC, negative control; CPR, NADPH-cytochrome P450 reductase; p-p38 MAPK, phosphorylated p38 mitogen-activated protein kinase; $A\beta_{1-42}$, 42-residue amyloid β protein fragment.

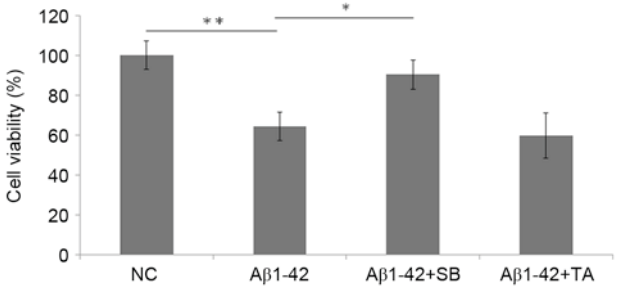

Figure 3. Inhibition of p38 mitogen-activated protein kinase promotes the viability of $A\beta_{1-42}$-treated SH-SY5Y cells. Cell viability in the NC group was set as 100%. $^{*}P<0.05$, $^{**}P<0.01$. NC, negative control; $A\beta_{1-42}$, 42-residue amyloid β protein fragment; SB, SB203580; TA, tannic acid.

Neuroblastoma cell $A\beta_{1-42}$-induced apoptosis is attenuated by p38 MAPK, but not CPR, inhibition. DAPI staining indicated that inhibition of p38 MAPK could protect SH-SY5Y cells from apoptosis caused by the neural toxicity of $A\beta_{1-42}$ (Fig. 4). Inhibition of CPR yielded no differences in the level of apoptosis (Fig. 4). The activity of caspase-3 was significantly increased following treatment with 10 μM $A\beta_{1-42}$ compared with the untreated cells (P<0.01; Fig. 4B). However, caspase-3 activity was significantly decreased in $A\beta_{1-42}$-treated cells after SB203580 treatment compared with cells treated with $A\beta_{1-42}$ alone (P<0.05; Fig 4A), while no changes were identified in the cells treated with $A\beta_{1-42}$ and TA. These results suggest that the inhibition of p38 MAPK protects SH-SY5Y cells from apoptosis.

p38 MAPK inhibition promotes contextual memory improvement. No significant differences were identified in relative memory deficit between the WT and SB203580 treated WT mice, suggesting that SB203580 is not toxic to normal cognitive function (data not shown). However, the AD mice demonstrated significant memory deficiencies compared with the WT mice (P<0.01; Fig. 5), indicating impaired contextual memory. Following the inhibition of p38 MAPK, the contextual memory of SB-treated AD mice significantly improved compared with untreated AD mice (P<0.05), although was still deficient compared with the WT mice (Fig. 5). These results suggest that the deficiency in contextual memory identified in AD mice is due to neural toxicity and could be improved by inhibition of p38 MAPK.

Discussion

AD is a chronic neurodegenerative disease for which there are no effective drug treatments. At present, the morbidity of AD is increasing worldwide. However, the mechanism of the development of AD remains unclear. The present study aimed to elucidate the role of p38 MAPK and CPR in AD, in animals and at the cellular level. The AD mouse model ASPswe/PSEN1dE9 encoding a chimeric Aβ (A4) precursor protein (APPswe) and mutation of human presenilin 1 was generated in the Jackson Laboratory. Thioflavin S staining was then applied to detect senile plaques. As neuritic deposits consisting of Aβ peptides, such as $A\beta_{1-42}$, in the cortex of the brain, senile plaques are variable in shape, area and size, and are associated with degenerative neural structures, and an abundance of microglia and astrocytes (16). Senile plaques, in which abnormal neurites are composed primarily of paired helical filaments and neurofibrillary tangles, are one of the most important characteristic features of AD. $A\beta_{1-42}$ tends to aggregate into senile plaques and is neurotoxic (16-18). The present study revealed that senile plaques were seldom identified in healthy mice in the WT group. The number of senile plaques was greater in the AD group, indicating that AD mice were successfully generated.

Using this AD mouse model, the expression of p38 MAPK was examined. p38 MAPK, also called cytokinin-specific binding protein, is the mammalian orthologue of the yeast protein, Hog1p MAP kinase. p38 MAPK is involved in a signaling cascade controlling cellular responses, similar to the stress-activated protein kinase/c-Jun N-terminal kinase signaling pathway (19). In the present study, p-p38 MAPK was demonstrated to be significantly upregulated in the brain cortex of mice in the AD group. p38 MAPK can be activated by a variety of cellular stressors. In a previous study by our group, p38 MAPK could be activated by inflammatory cytokines, lipopolysaccharides and growth factors in mice brains (unpublished). This previous study indicated that the inflammation was induced and p38 MAPK was involved in AD. Whether the inflammation in the brain was primarily induced through the p38 MAPK signaling pathway remains unclear and requires further study. The conclusion from the previous study by our group was investigated in the present study by experiments on the human SH-SY5Y neuroblastoma cell line, whose original cell line, SK-N-SH, was isolated from a bone marrow biopsy obtained from a 4-year-old female with

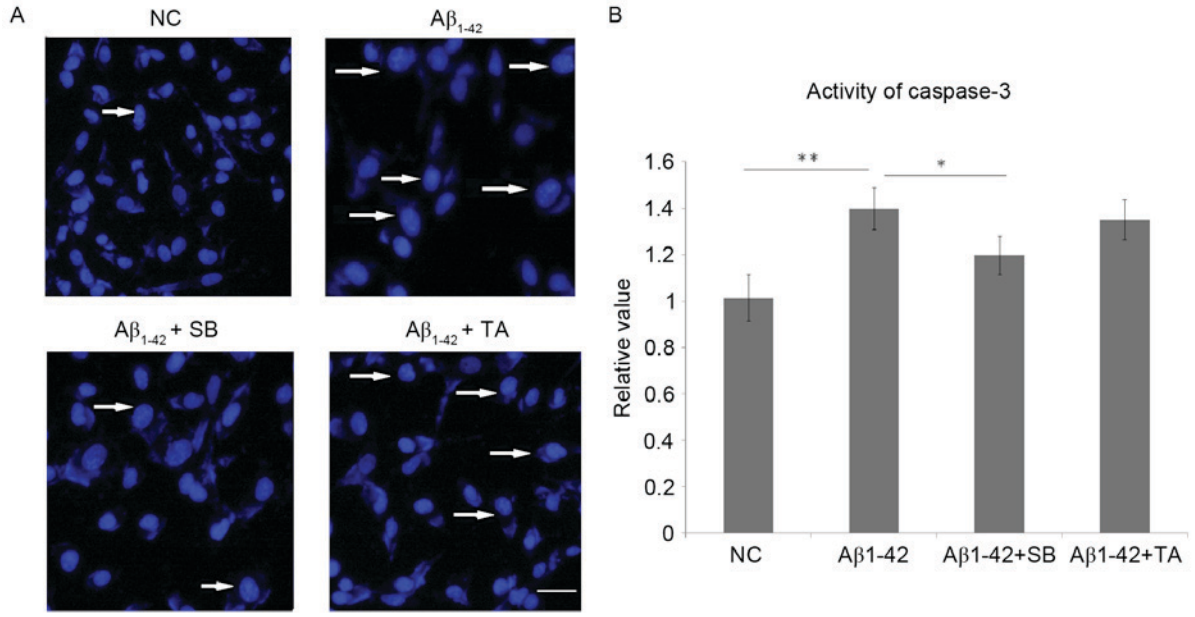

Figure 4. $A\beta_{1-42}$-induced apoptosis is attenuated by p38 mitogen-activated protein kinase inhibition. (A) Apoptosis was detected using DAPI staining (apoptotic bodies are indicated by white arrows). Scale bar, 50 μm; magnification, x200. (B) The activity of caspase-3 was used to quantify the level of apoptosis in the four groups. *P<0.05, **P<0.01. NC, negative control; $A\beta_{1-42}$, 42-residue amyloid β protein fragment; SB, SB203580; TA, tannic acid.

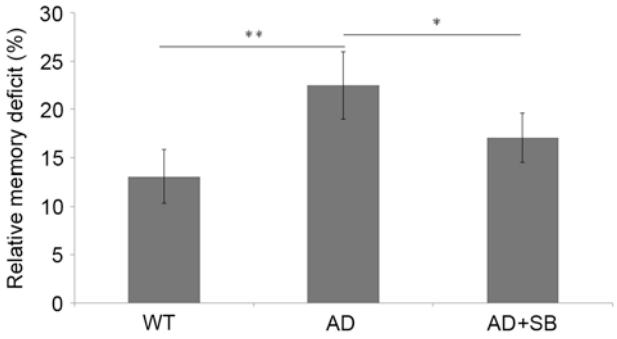

Figure 5. p38 mitogen-activated protein kinase inhibition attenuates contextual memory deficiencies in AD mice. Relative memory deficit was calculated as the percentage of freezing. *P<0.05, **P<0.01. WT, wild-type; SB, SB203580; AD, Alzheimer's disease.

neuroblastoma. SH-SY5Y cells are widely used for *in vitro* neuronal function and differentiation studies. Given that AD is a human neurodegenerative disease, these human cells were selected instead of mouse neurons.

Aβ peptides are formed through sequential cleavage of the amyloid precursor protein. $A\beta_{1-42}$ is associated with AD; thus, $A\beta_{1-42}$ was used as a neural toxin to treat the SH-SY5Y cells. The present study identified that p-p38 MAPK was significantly upregulated in SH-SY5Y cells treated with $A\beta_{1-42}$, indicating that p38 MAPK is a potential target for the treatment of AD.

Another important enzyme in AD, CPR, was investigated in the current study. CPR, a microsomal flavoprotein and redox partner of CYPs, is required for all monooxygenase reactions catalyzed by microsomal CYPs, shuttling electrons from NADPH into the iron of the prosthetic heme group of CYPs through FAD and FMN coenzymes (20). CPR is located in the inner membrane of the mitochondria and in the endoplasmic reticulum of cells, and is present in the majority of tissues of the body, such as the brain, metabolizing thousands of endogenous and exogenous chemicals. CPR is one of the main drug-metabolizing enzymes in the human body. Given that the aim of the present study was to evaluate the potential to target p38 MAPK in the treatment of AD, the role of CPR was also studied. A previous study from our group indicated that CPR was highly associated with astrocytosis (21). Along with p38 MAPK, CPR was also significantly upregulated in the cortex of mice in the AD group. However, the inhibition of CPR in SH-SY5Y cells indicated no significant difference compared with the cells treated with $A\beta_{1-42}$ alone. Thus, the role of CPR in the regulation of AD appears to be complex.

Given that p-p38 MAPK and CPR levels were increased in the cortexes of the brains of mice in the AD group and SH-SY5Y cells treated with $A\beta_{1-42}$, p38 MAPK and CPR were downregulated by inhibitor treatment in order to investigate their effect on cell viability and apoptosis. MTT assays were performed to analyze the viability of SH-SY5Y cells. Due to its neural toxicity, $A\beta_{1-42}$ significantly inhibited cell viability. Inhibition of p38 MAPK promoted the viability of SH-SY5Y cells treated with $A\beta_{1-42}$. DAPI staining also confirmed that inhibition of p38 MAPK protected SH-SY5Y cells from apoptosis caused by the neural toxicity of $A\beta_{1-42}$. Inhibition of CPR demonstrated no significant benefits to cellular viability or apoptosis. To confirm this effect, the activity of caspase-3, which is activated in apoptotic cells and serves as a key indicator for apoptosis, was analyzed. Caspase-3 was significantly increased in SH-SY5Y cells that were treated with $A\beta_{1-42}$ and significantly decreased following the inhibition of p38 MAPK. However, CPR inhibition demonstrated no significant effect on apoptosis.

Based on the *in vitro* experiments performed in the present study, *in vivo* experiments were conducted. A fear-conditioning assay was performed to determine the contextual memory of the mice, since contextual memory deficiency is one of the

main symptoms of AD (22). Due to neural toxicity, deficiencies in contextual memory were identified in AD mice. Notably, inhibition of p38 MAPK was revealed to improve contextual memory in AD mice.

In conclusion, the results of the present study indicate that p38 MAPK is overactive in AD. CPR was also involved in this process; however, its activity in the regulation of AD was more complex than p38 MAPK. Due to neural toxicity, the number of senile plaques increased and deficiencies in contextual memory were identified in the AD mice. These symptoms were reduced by p38 MAPK inhibition. Inhibition of p38 MAPK was also demonstrated to protect $A\beta_{1-42}$-treated SH-SY5Y cells from apoptosis and promote their viability. These findings provide novel insights into the pathogenesis of AD and highlight potential targets for AD treatment.

Acknowledgements

The present study was supported by the Natural Science Foundation of Jiangsu Province (grant no. BK20130219), the National Nature Science Foundation of China (grant no. 81401045) and the Qing Lan Project of Jiangsu Province.

References

1. Shampo MA, Kyle RA and Steensma DP: Alois Alzheimer-Alzheimer disease. Mayo Clin Proc 88: e155, 2013.
2. Alzheimer's Association: 2017 Alzheimer's disease facts and figures. Alzheimers Dement 13: 325-373, 2017.
3. Nithianantharajah J and Hannan AJ: The neurobiology of brain and cognitive reserve: Mental and physical activity as modulators of brain disorders. Prog Neurobiol 89: 369-382, 2009.
4. Arbor SC, LaFontaine M and Cumbay M: Amyloid-beta Alzheimer targets-protein processing, lipid rafts, and amyloid-beta pores. Yale J Biol Med 89: 5-21, 2016.
5. Su F, Bai F and Zhang Z: Inflammatory cytokines and Alzheimer's disease: A review from the perspective of genetic polymorphisms. Neurosci Bull 32: 469-480, 2016.
6. Lénárt N, Brough D and Dénes Á: Inflammasomes link vascular disease with neuroinflammation and brain disorders. J Cereb Blood Flow Metab 36: 1668-1685, 2016.
7. Hall JR, Wiechmann AR, Johnson LA, Edwards M, Barber RC, Cunningham R, Singh M and O'Bryant SE: Total cholesterol and neuropsychiatric symptoms in Alzheimer's disease: The impact of total cholesterol level and gender. Dement Geriatr Cogn Disord 38: 300-309, 2014.
8. Rea R, Carotenuto A, Fasanaro AM, Traini E and Amenta F: Apathy in Alzheimer's disease: Any effective treatment? ScientificWorldJournal 2014: 421385, 2014.
9. Zheng C, Zhou XW and Wang JZ: The dual roles of cytokines in Alzheimer's disease: Update on interleukins, TNF-α, TGF-β and IFN-γ. Transl Neurodegener 5: 7, 2016.
10. Tompkins LM and Wallace AD: Mechanisms of cytochrome P450 induction. J Biochem Mol Toxicol 21: 176-181, 2007.
11. Souslova T, Marple TC, Spiekerman AM and Mohammad AA: Personalized medicine in Alzheimer's disease and depression. Contemp Clin Trials 36: 616-623, 2013.
12. Lu J, Wan L, Zhong Y, Yu Q, Han Y, Chen P, Wang B, Li W, Miao Y and Guo C: Stereoselective metabolism of donepezil and steady-state plasma concentrations of S-donepezil based on CYP2D6 polymorphisms in the therapeutic responses of Han Chinese patients with Alzheimer's disease. J Pharmacol Sci 129: 188-195, 2015.
13. Yan H, Kong Y, He B, Huang M, Li J, Zheng J, Liang L, Bi J, Zhao S and Shi L: CYP2J2 rs890293 polymorphism is associated with susceptibility to Alzheimer's disease in the Chinese Han population. Neurosci Lett 593: 56-60, 2015.
14. Mast N, Li Y, Linger M, Clark M, Wiseman J and Pikuleva IA: Pharmacologic stimulation of cytochrome P450 46A1 and cerebral cholesterol turnover in mice. J Biol Chem 289: 3529-3538, 2014.
15. Bolivar VJ, Manley K and Messer A: Exploratory activity and fear conditioning abnormalities develop early in R6/2 Huntington's disease transgenic mice. Behav Neurosci 117: 1233-1242, 2003.
16. Mohri I, Kadoyama K, Kanekiyo T, Sato Y, Kagitani-Shimono K, Saito Y, Suzuki K, Kudo T, Takeda M, Urade Y, *et al*: Hematopoietic prostaglandin D synthase and DP1 receptor are selectively upregulated in microglia and astrocytes within senile plaques from human patients and in a mouse model of Alzheimer disease. J Neuropathol Exp Neurol 66: 469-480, 2007.
17. Nathalie P and Jean-Noël O: Processing of amyloid precursor protein and amyloid peptide neurotoxicity. Curr Alzheimer Res 5: 92-99, 2008.
18. Iqbal K and Grundke-Iqbal I: Alzheimer neurofibrillary degeneration: Significance, etiopathogenesis, therapeutics and prevention. J Cell Mol Med 12: 38-55, 2008.
19. Kashimata M, Sayeed S, Ka A, Onetti-Muda A, Sakagami H, Faraggiana T and Gresik EW: The ERK-1/2 signaling pathway is involved in the stimulation of branching morphogenesis of fetal mouse submandibular glands by EGF. Dev Biol 220: 183-196, 2000.
20. Laursen T, Jensen K and Møller BL: Conformational changes of the NADPH-dependent cytochrome P450 reductase in the course of electron transfer to cytochromes P450. Biochim Biophys Acta 1814: 132-138, 2011.
21. Yao Y, Liu S, Wang Y, Yuan W, Ding X, Cheng T, Shen Q and Gu J: Suppression of cytochrome P450 reductase expression promotes astrocytosis in subventricular zone of adult mice. Neurosci Lett 548: 84-89, 2013.
22. Webster SJ, Bachstetter AD, Nelson PT, Schmitt FA and Van Eldik LJ: Using mice to model Alzheimer's dementia: An overview of the clinical disease and the preclinical behavioral changes in 10 mouse models. Front Genet 5: 88, 2014.